

## Fermi level pinning and chemical interactions at metal-In x Ga1-x As(100) interfaces

L. J. Brillson, M. L. Slade, R. E. Viturro, M. K. Kelly, N. Tache, G. Margaritondo, J. M. Woodall, P. D. Kirchner, G. D. Pettit, and S. L. Wright

Citation: *Journal of Vacuum Science & Technology B* **4**, 919 (1986); doi: 10.1116/1.583537

View online: <http://dx.doi.org/10.1116/1.583537>

View Table of Contents: <http://scitation.aip.org/content/avs/journal/jvstb/4/4?ver=pdfcov>

Published by the AVS: Science & Technology of Materials, Interfaces, and Processing

## Instruments for advanced science

### Gas Analysis



- dynamic measurement of reaction gas streams
- catalysis and thermal analysis
- molecular beam studies
- dissolved species probes
- fermentation, environmental and ecological studies

### Surface Science



- UHV TPD
- SIMS
- end point detection in ion beam etch
- elemental imaging - surface mapping

### Plasma Diagnostics



- plasma source characterization
- etch and deposition process reaction kinetic studies
- analysis of neutral and radical species

### Vacuum Analysis



- partial pressure measurement and control of process gases
- reactive sputter process control
- vacuum diagnostics
- vacuum coating process monitoring

contact Hiden Analytical for further details

**HIDEN**  
ANALYTICAL

[info@hideninc.com](mailto:info@hideninc.com)

[www.HidenAnalytical.com](http://www.HidenAnalytical.com)

CLICK to view our product catalogue



# Fermi level pinning and chemical interactions at metal-In<sub>x</sub>Ga<sub>1-x</sub>As(100) interfaces

L. J. Brillson, M. L. Slade, and R. E. Viturro  
*Xerox Webster Research Center, Webster, New York 14580*

M. K. Kelly, N. Tache, and G. Margaritondo  
*Physics Department, University of Wisconsin-Madison, Madison, Wisconsin 53706*

J. M. Woodall, P. D. Kirchner, G. D. Pettit, and S. L. Wright  
*IBM Thomas J. Watson Research Center, Yorktown Heights, New York 10598*

(Received 29 January 1986; accepted 24 March 1986)

Soft x-ray photoemission spectroscopy (SXPS) measurements of metals on clean, ordered In<sub>x</sub>Ga<sub>1-x</sub>As(100) surfaces reveal that Fermi level stabilization energies depend strongly on the particular metal, i.e., the Fermi level is not pinned. For In<sub>x</sub>Ga<sub>1-x</sub>As,  $x > 0$ , the range of Fermi level movement is comparable to or greater than the semiconductor band gap. For the same metal on different alloys, we observe regular trends in stabilization energies. The trend for Au is strikingly different from previous, air-exposed values. Our results challenge Schottky barrier models based on simple native defects, metal-induced gap states, or the "common-anion" rule. Observed variations in semiconductor outdiffusion provide a chemically-modified interface work function model which accounts for the data across the alloy series.

## I. INTRODUCTION

The mechanisms by which Schottky barriers form at metal/III-V compound semiconductor interfaces has been of considerable interest over the past two decades because of the apparently weak dependence of the band bending on different metal contacts.<sup>1,2,3</sup> This insensitivity presents serious difficulties to the designer of GaAs-based high-speed and optoelectronic devices.<sup>4</sup> Historically, fundamental studies of Schottky barrier formation on III-V compounds have been directed primarily at GaAs and its (110) cleavage face in particular. In this case, the energy at which the surface Fermi level  $E_F$  stabilizes appear to be relatively insensitive to the chemical nature of the metal contact or to ambient contamination, falling into the range of only a few tenths of eV near the center of the GaAs band gap.<sup>5,6</sup> To account for this "pinning" behavior, researchers have proposed a variety of microscopic models, including gap states due to defects formed by metal atom condensation,<sup>7</sup> metal-induced gap states defined by the semiconductor band structure<sup>8</sup> or by chemisorption and charge transfer involving metal atoms and clusters,<sup>9</sup> chemically-formed dipole layers,<sup>10</sup> and effective work functions of interface alloys involving As precipitates.<sup>11,12</sup> Studies of InP(110)<sup>13,14</sup> and GaAs(100)<sup>13</sup> suggest that a somewhat wider range of  $E_F$  gap positions are possible. Nevertheless, it is not yet clear whether the nature of the metal contact has a major or minor influence for the III-V compounds in general.

The electrical behavior of the ternary alloy series In<sub>x</sub>Ga<sub>1-x</sub>As has until now been used to support a defect pinning model of Schottky barrier formation with a narrow range of  $E_F$  stabilization energies.<sup>16-20</sup> The data are based upon capacitance versus voltage ( $C-V$ ) measurements on Schottky barrier diodes<sup>21</sup> and gate-controlled galvanometric measurements on metal-insulator semiconductor (MIS) capacitor and transistor test structures.<sup>22</sup> The metal-semiconductor experiments were performed on air-exposed,

etched In<sub>x</sub>Ga<sub>1-x</sub>As(100) surfaces with Au contacts.<sup>21</sup> The agreement between these data and theoretical calculations of anion vacancies,<sup>17</sup> antisite (cation replacing anion) defects,<sup>18,19</sup> or cation dangling bonds<sup>20</sup> have been used to argue for defects as the cause of the  $E_F$  "pinning."

In this paper, we report on the initial stages of Schottky barrier formation for metal deposition on clean, ordered surfaces of In<sub>x</sub>Ga<sub>1-x</sub>As under ultrahigh vacuum (UHV) conditions. Soft x-ray photoemission spectroscopy (SXPS) measurements of rigid shifts in core level spectra demonstrate that the surface  $E_F$  stabilizes at energies which depend strongly on the particular metal. For  $x > 0$ , the range of  $E_F$  movement and the resultant band bending is comparable to or greater than the semiconductor band gap. For the same metal on different alloys, we observe regular trends in  $E_F$  overlayer on  $E_F$  position and the specific trends across the alloy series strongly challenge Schottky barrier models based on simple vacancy or antisite defects as well as the common-anion rule of III-V barrier formation. Instead, SXPS measurements of semiconductor outdiffusion reveal significant changes in near-interface composition between different metal-semiconductor systems and suggest that chemical modification of the interface leads to a range of metal-alloy compositions whose work functions determine the barrier formation.

## II. EXPERIMENTAL

The study of clean, ordered GaInAs surfaces is complicated by the absence of bulk single crystals for cleaving in UHV. We circumvented this problem by growing thick films by molecular beam epitaxy (MBE), then "capping" the freshly grown film with several thousand monolayers of As. In all cases reported here, In<sub>x</sub>Ga<sub>1-x</sub>As layers 7500 Å thick ( $n = 5 \times 10^{16}$  Si/cm<sup>3</sup>) were grown over 2000 Å In<sub>x</sub>Ga<sub>1-x</sub>As ( $n = 10^{19}$ /cm<sup>3</sup>) and on top of 1000 Å GaAs ( $n = 10^{19}$ /cm<sup>3</sup>) and an  $n^+$  GaAs(100) substrate. This mul-

tilayer film structure yielded an unstrained  $\text{In}_x\text{Ga}_{1-x}\text{As}(100)$  outer film and an Ohmic contact through the degenerately-doped base layers and substrate. By desorbing the As "cap" under high vacuum conditions,<sup>23</sup> we obtain a clean and ordered  $(1 \times 1)$  surface as determined from valence band photoemission spectroscopy and low energy electron diffraction (LEED), respectively. Even though the resultant surface is likely to be As-stabilized,<sup>24</sup> a comparison of surface versus bulk-sensitive SXPS core level intensities revealed no apparent excess of surface As. For example, As  $3d$ /Ga  $3d$  core level intensity ratios were compared for photoelectron kinetic energies of 50–100 eV (surface-sensitive<sup>25</sup>) versus 10–20 eV (bulk-sensitive) using appropriate excitation energies. They showed no systematic deviations with depth sensitivity.

The energies of SXPS spectral features appear reproducibly from surface to surface of the same alloy concentration and the energies vary systematically with different compositions across the alloy series. For each alloy composition, the SXPS core level peaks and valence band edge are reproducible to within  $\pm 0.05$  and  $\pm 0.15$  eV, respectively. Assuming the same  $E_F$  position with respect to the band edges for each clean alloy (for  $n = 5 \times 10^{16}/\text{cm}^3$ ,  $E_c - E_F \sim 0.1$  eV), the SXPS valence band edges exhibit the correct decrease in band gap<sup>26</sup> with increasing In composition to within  $\pm 0.17$  eV. A valence band spectrum of a thick (220 Å) Au film deposited on InAs established the initial  $E_F$  position of clean InAs to be  $E_c - E_F = 0.1$  eV. Metal evaporation took place in a UHV chamber (base pressure  $P = 8 \times 10^{-11}$  Torr) from W filaments with a pressure rise no higher than mid- $10^{-9}$  Torr. A quartz crystal oscillator monitored the thin film depositions.

### III. RESULTS

We have measured the SXPS peak energies and intensities for the Ga  $3d$ , In  $4d$ , and As  $3d$  core levels as a function of Au, In, Al, and Ge deposition on  $\text{In}_x\text{Ga}_{1-x}\text{As}(100)$  surfaces, where  $x = 0, 0.25, 0.50, 0.75,$  and  $1.00$ . We obtained bulk-sensitive spectra in order to monitor core level shifts while minimizing line shape changes due to chemical bonding effects near the surface. In this case, we used  $h\nu = 40$  eV for the Ga  $3d$  and In  $4d$  spectra and  $h\nu = 60$  eV for the As  $3d$  spectra in order to produce photoelectrons in the 10–20 eV kinetic energy range. Figure 1 illustrates these core level shifts for Au deposition on clean  $\text{In}_{0.5}\text{Ga}_{0.5}\text{As}$ . The rigid shift to higher kinetic energy corresponds to an  $E_F$  movement of 0.3 eV toward the valence band maximum  $E_v$ . In general the sharp In  $4d$  and Ga  $3d$  peak features provide a clearer indication of  $E_F$  movement than the As  $3d$  feature. In many cases such as that of Fig. 1, the As  $3d$  peak feature becomes distorted by multiple components with different chemical bonding, even for the bulk-sensitive spectra. We also obtained surface-sensitive spectra in order to monitor outdiffusion of dissociated semiconductor species as well as chemical bonding changes of the metal adsorbates. Here, we used  $h\nu = 80$  eV for the Ga  $3d$  and In  $4d$  spectra and  $h\nu = 100$  eV for the As  $3d$  spectra in order to obtain photoelectrons in the 50–60 eV kinetic energy range. Integrated peak areas for the semiconductor constituents at the free

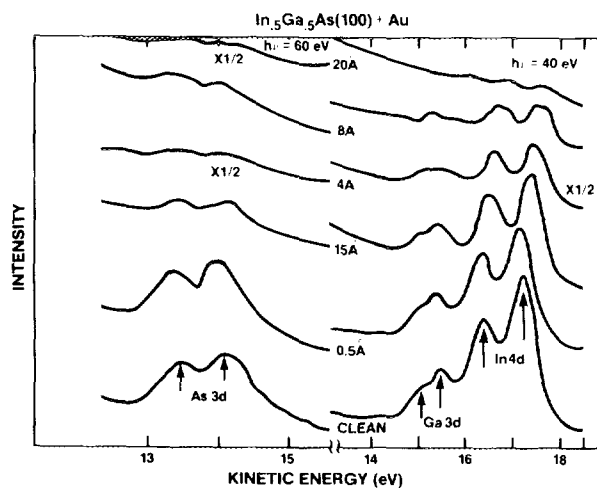


FIG. 1. SXPS core level spectra for As  $3d$  at  $h\nu = 60$  eV and Ga  $3d$  and In  $4d$  at  $40$  eV as a function of increasing Au deposition. Arrows indicate spin-orbit split components. The rigid core level shifts provide a measure of  $E_F$  movement relative to the band edges.

metal surface provide a measure of the change in stoichiometry at the metal–semiconductor interface.

Line shape changes also reveal the presence of dissociated species. Thus, for Au on  $\text{In}_{0.5}\text{Ga}_{0.5}\text{As}$ , surface-sensitive spectra (not shown) display a dissociated As  $3d$  feature displaced to higher binding energy, corresponding to As outdiffusion. In general, core level shifts in  $4d$  and Ga  $3d$  peak for substrate features in the surface-sensitive spectra were in agreement with those of the corresponding bulk-sensitive spectra.

The  $E_F$  movements induced by metal deposition on  $\text{In}_x\text{Ga}_{1-x}\text{As}(100)$  indicate a wide range of Schottky barrier positions for each of the In alloys. Figure 2 illustrates the different  $E_F$  behavior produced by Au, Al, and In deposition on  $\text{In}_{0.25}\text{Ga}_{0.75}\text{As}(100)$ . Each metal exhibits a different  $E_F$  movement with increasing metal coverage. The thickness over which each curve approaches an asymptotic value is in all cases more than one or two monolayers. Differences in the rate, sign, and magnitude of  $E_F$  movement are apparent, indicative of differences in the chemical interaction between metal and semiconductor. At 20 Å metal coverage, the final  $E_F$  positions extend from 0.25 eV above  $E_c$  to 0.42 eV below  $E_c$ ; an energy range of 0.67 eV compared to the band gap of 1.05 eV.<sup>26</sup>

Differences between metals are even more apparent for  $E_F$  movement on clean InAs(100) surfaces, as shown in Fig. 3. At 20 Å metal coverage, the final  $E_F$  positions extend from 0.1 eV above  $E_c$  to 0.14 eV below  $E_c$ ; a range of 0.6 eV compared to the InAs band gap of 0.36 eV.<sup>26</sup> Furthermore, the  $E_F$  stabilization positions for Al, In, Ge, and Au appear to be distributed in energy, rather than clustered around particular positions. Analogous plots for other alloy semiconductors yield ranges of 0.85 eV for  $\text{In}_{0.75}\text{Ga}_{0.25}\text{As}$  ( $E_g = 0.53$  eV) and 0.65 eV for  $\text{In}_{0.50}\text{Ga}_{0.50}\text{As}$  ( $E_g = 0.76$  eV). For GaAs, we studied only Au and In overlayers on GaAs(100), which yielded a range of  $\sim 0.4$  eV ( $E_g = 1.43$  eV). Thus, moving away from GaAs, one obtains larger ranges of  $E_F$  movement which are comparable to or larger than the semiconductor band gap.

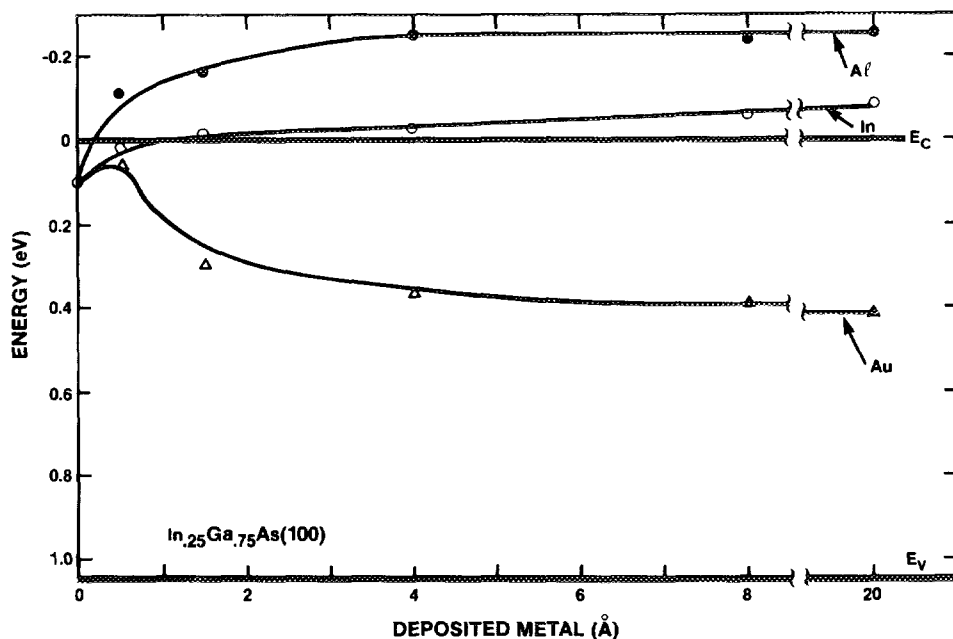


FIG. 2. Fermi level movements for clean  $\text{In}_{0.25}\text{Ga}_{0.75}\text{As}(100)$  (band gap = 1.05 eV) as a function of Au, In, or Al deposition in ultrahigh vacuum.

The  $E_F$  stabilization energies obtained by SXPS show large differences for clean  $\text{In}_x\text{Ga}_{1-x}\text{As}(100)$  surfaces with and without subsequent air exposure. For this comparison, we exposed thermally-cleaned  $\text{InGaAs}(100)$  surfaces to 50 Torr air (10 Torr  $\text{O}_2$ ) for 100 s in a stainless steel reaction chamber attached to the UHV analysis chamber. No hot filaments were present. For the same initially clean  $\text{InAs}(100)$  surface, Fig. 4(a) illustrates a striking difference in  $E_F$  behavior between air-exposed versus clean cases with Au deposition. The immediate effect of air exposure is to move  $E_F$  up into the conduction band. Whereas  $E_F$  for the clean surface moves down into the valence band,  $E_F$  for the air-exposed surface remains near the conduction band edge. Figure 4(b) provides an example for which air exposure produces the opposite shift with respect to the clean interface. Here initial air exposure shifts  $E_F$  down into the band gap where it remains with In deposition. In contrast,  $E_F$  for the clean surface rises into the conduction band with In coverage. Significantly, the  $E_F$  positions for the two air-exposed cases shown in Fig. 4 are in agreement with the electrical data of Kayiyama,<sup>21</sup> which were based on air-exposed material.

Recently, Baier *et al.*<sup>27</sup> have measured an  $E_F$  position of

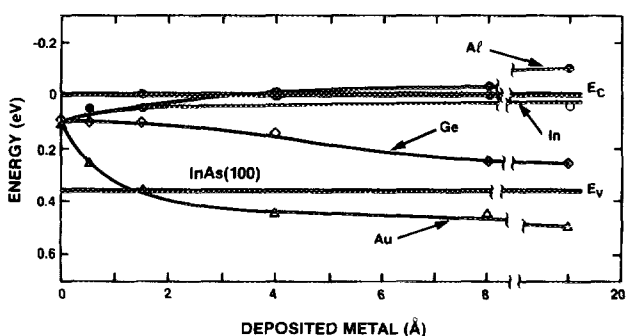


FIG. 3. Fermi level movements for clean  $\text{InAs}(100)$  (band gap = 0.36 eV) as a function of Au, In, Ge, or Al deposition in ultrahigh vacuum.

J. Vac. Sci. Technol. B, Vol. 4, No. 4, Jul/Aug 1986

0.13 eV above the conduction band edge for both cleaved and oxidized  $\text{InAs}(110)$ . The difference between our clean  $\text{InAs}(100)$  and the cleaved (110) result is most likely due to different surface preparations, i.e., As passivation and subsequent reevaporation for (100) MBE-grown versus cleavage for (110) melt-grown  $\text{InAs}$ .  $\text{GaAs}(100)$  MBE-grown and (110) melt-grown surfaces exhibit analogous differences in  $E_F$  movement.<sup>28</sup>

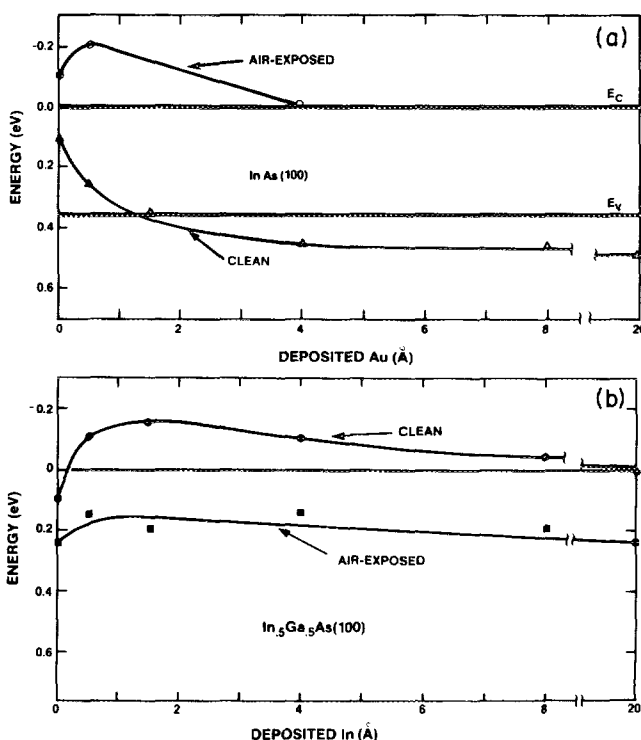


FIG. 4. Fermi level movements for (a) clean and air-exposed  $\text{InAs}(100)$  as a function of Au deposition and (b) clean and air-exposed  $\text{In}_{0.5}\text{Ga}_{0.5}\text{As}(100)$  as a function of In deposition. Clean semiconductor surfaces provide the starting point in all cases.

#### IV. DISCUSSION

The  $E_F$  stabilization energies for Au, Al, In, and Ge on clean  $\text{In}_x\text{Ga}_{1-x}\text{As}(100)$ ,  $0 < x < 1$  surfaces provide sufficient data to evaluate the applicability of various Schottky barrier models. In Fig. 5, the energy levels for the entire InGaAs alloy series are plotted relative to the GaAs valence band maximum (left-hand scale) and to the vacuum level (right-hand scale). The valence band edges of InAs and GaAs are determined from photoemission threshold measurements of van Laar *et al.*<sup>29</sup> (e.g., 5.42 eV for InAs and 5.56 eV for GaAs). The small difference  $\Delta E_v$  between the two alloy extrema allow us to approximate  $E_v$  at intermediate alloy compositions by a linear ramp. On the other hand, the compositional dependence of the lowest energy direct gaps measured by electroreflectance<sup>26</sup> indicates a distinct bowing, which is indicated in Fig. 5 by the curvature of the conduction band edge. The data points are in reasonable agreement with what little results have been measured previously for clean metal– $\text{In}_x\text{Ga}_{1-x}\text{As}$  interfaces. For Au on GaAs(100), Grant *et al.* measured  $E_c - E_F = 0.75$  eV (versus 0.75 eV in Fig. 5) as well as a range of  $E_c - E_F$  energies ranging from 0.75 to 0.2 eV with surface treatment.<sup>15</sup> For In on GaAs(100), the high position ( $E_c - E_F = 0.35$  eV) relative to that of Au agrees with SXPS work of Daniels *et al.*<sup>30</sup> for cleaved GaAs(110) (e.g., 0.4 vs 0.9 eV<sup>7</sup>). Schottky barrier height data for MBE-grown Al on  $n\text{-In}_{0.5}\text{Ga}_{0.5}\text{As}(100)$  also support the SXPS results, exhibiting Ohmic behavior<sup>31</sup> (e.g.,  $E_c - E_F < 0$ ).

The first conclusion reached upon inspection of the wide  $E_F$  ranges in Fig. 5 is that  $E_F$  is not “pinned.” These large energy differences with metals are inconsistent with models based on pinning in a narrow energy range, where the effect of the metal is secondary. Included are the unified defect model involving high densities of closely-spaced defect energy levels<sup>7</sup> and metal-induced state pinning at a mid-gap position defined primarily by the semiconductor band structure.<sup>8</sup> In fact, the metal-induced gap state model leads to a large error for the Au–InAs  $E_F$  position,<sup>8</sup> even after taking the metal electronegativity and band structure effects (i.e., spin-orbit splitting, in direct gaps) into account. It should be emphasized that the  $E_F$  ranges for each semiconductor com-

position in Fig. 5 are internally consistent. They each involve clean surfaces of the same material with the same starting position for  $E_F$  with respect to the band edges.

For a given metal on different alloy semiconductors, the  $E_F$  stabilization positions follow regular trends as indicated by the fitted curves in Fig. 5. Besides exhibiting a sizable variation in energy, each curve appears to parallel the conduction band, especially In and Al. These movements are contrary to theoretical calculations of native defects reported thus far. Simple vacancies,<sup>17</sup> anion-on-cation antisite defects,<sup>18,19</sup> and cation dangling bonds<sup>20</sup> all display trends which parallel the valence rather than the conduction band and which lie above the conduction band for  $x_{\text{In}} < 0.5$ . Within a localized state model, the conduction band trends may be consistent only with cation-derived bulk states. The strong variation of  $E_F$  with respect to the valence band both for the same metal with different alloys and for different metals on the same alloy argues conclusively against a “common-anion rule.”<sup>32</sup> In this model, the same  $E_F - E_v$  would have to appear for all III–V compounds with the same anion. Finally, the conduction band trends in Fig. 5 do not support an anion work function dominated, for example, by As precipitates. In this case,  $E_F$  energies would also be at constant energies below the vacuum level.

One possible explanation of our data invokes defect levels which are widely spaced and of variable density.<sup>23,33</sup> Studies of  $\text{Ga}_{0.47}\text{In}_{0.53}\text{As}$  MIS structures suggest that the densities of any interface states on dielectric-coated GaInAs surfaces are relatively low and are further reduced by thermal annealing.<sup>22,34,35</sup> The observed  $E_F$  excursions in  $C$ – $V$  and field-effect-controlled galvanomagnetic measurements are interpreted in terms of the position and density of donor and acceptor levels near the interface. It can be argued that the adsorbates whose  $E_F$  behavior is at variance with defect pinning represent special cases which result from chemical modification of the interface. In fact, such cases represent the rule rather than the exception.<sup>3</sup>

Without invoking localized interface states, it is possible to account for the observed  $E_F$  stabilization energies in terms of differences in overlayer work function due to changes in interface chemical composition. SXPS core level intensities provide a measure of the relative composition of outdiffusion species to the free metal surface and, by extension, a measure of the stoichiometry at the metal–semiconductor interface. For Au on  $\text{In}_x\text{Ga}_{1-x}\text{As}(100)$  and increasing  $x_{\text{In}}$ , the SXPS spectra indicate an increasing proportion of dissociated As, i.e., a trend from an As-rich to an As-deficient interface.<sup>23</sup> Assuming that the interface work function varies from  $\varphi_{\text{As}} \sim 4.8^{12}$  eV to  $\varphi_{\text{Au}} = 5.2$ – $5.4$  eV<sup>36</sup> under these conditions, the resultant trend agrees with the Au data points in Fig. 5 both in range and in absolute values. For In on  $\text{In}_x\text{Ga}_{1-x}\text{As}(100)$ , we observe a chemical trend from a As-deficient to an As-rich interface with increasing  $x_{\text{In}}$ .<sup>23</sup> These values agree with the In points in Fig. 5 in range, although their absolute values appear to be 0.1–0.2 eV too low. The In–GaAs(100) point may deviate from the otherwise near-linear trend in part because of the absence of lower- $\varphi$  In vs Ga at the interface.<sup>36</sup> For Al on  $\text{In}_x\text{Ga}_{1-x}\text{As}(100)$ , As accumulation at the interface in-

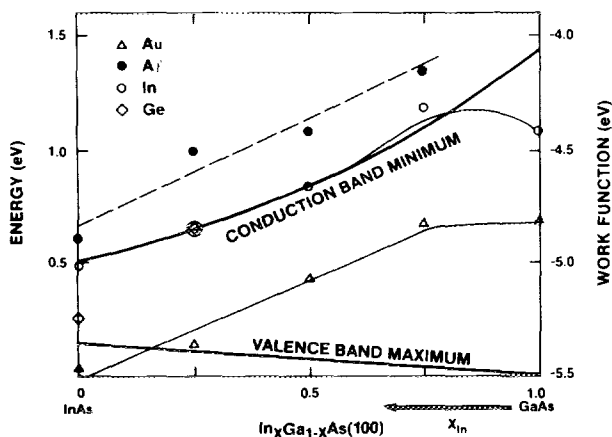


FIG. 5. Fermi level stabilization energies for Au, In, Ge, and Al deposited on clean  $\text{In}_x\text{Ga}_{1-x}\text{As}(100)$ ,  $0 < x < 1$ , in ultrahigh vacuum. Left (right)-hand scale is relative to the GaAs valence band maximum (the vacuum level).

creases with  $x_{\text{In}}$ .<sup>23</sup> For GaAs, this As may be bound up as reacted AlAs, with a work function different from  $\varphi_{\text{As}}$ . With additional accumulation, the excess As may form precipitates, thereby dominating the interface work function. Given  $\varphi_{\text{Al}} \sim 4.2$  eV,<sup>36</sup> the variation in local  $\varphi$  may then approximate that of In. Hence by using observations of interface chemical compositions and a classical work function model, we are able to account for a large set of interface data on both an absolute and relative scale.

## V. CONCLUSIONS

We have performed (the first) SXPS core level measurements for metals on clean, ordered surfaces of a ternary III-V compound semiconductor  $\text{In}_x\text{Ga}_{1-x}\text{As}(100)$ . We find that the Fermi level exhibits no pinning across the entire In alloy series. Air exposure of the clean ternary surfaces prior to metal deposition produces major changes in the subsequent  $E_F$  level movements. The wide variations in  $E_F$  stabilization energy for different metals on the same semiconductor as well as the same metal across the alloy series preclude a number of leading Schottky barrier models. Chemically-modified changes in metal-alloy composition rather than interface defects levels appear to be the most straightforward explanation for the barrier formation at  $\text{In}_x\text{Ga}_{1-x}\text{As}(100)$ -metal interfaces.

## ACKNOWLEDGMENTS

We gratefully acknowledge partial support by the Office of Naval Research Contract No. ONR N00014-80-C-0778. The Synchrotron Radiation Center is supported by the National Science Foundation. We wish to give particular thanks to the staff of the Aladdin Storage Ring Facility for their outstanding efforts in implementing these experiments.

<sup>1</sup>C. A. Mead, *Solid State Electron.* **9**, 1023 (1966).

<sup>2</sup>S. M. Sze, *Physics of Semiconductor Devices*, 2nd ed. (Wiley-Interscience, New York, 1981), Chap. 5.

<sup>3</sup>L. J. Brillson, *Surf. Sci. Rep.* **2**, 123 (1982).

<sup>4</sup>A. G. Milnes, *Semiconductor Devices and Integrated Electronics* (Van Nostrand Reinhold, New York, 1980).

<sup>5</sup>I. Lindau, P. W. Chye, C. M. Garner, P. Pianetta, C. Y. Su, and W. E. Spicer, *J. Vac. Sci. Technol.* **15**, 1332 (1978).

<sup>6</sup>W. E. Spicer, I. Lindau, P. Skeath, C. Y. Su, and P. W. Chye, *Phys. Rev. Lett.* **44**, 420 (1980).

<sup>7</sup>W. E. Spicer, I. Lindau, P. Skeath, and C. Y. Su, *J. Vac. Sci. Technol.* **17**, 1019 (1980).

<sup>8</sup>J. Tersoff, *Phys. Rev. B* **32**, 6968 (1985); *Phys. Rev. Lett.* **52**, 465 (1984); *J. Vac. Sci. Technol. B* **3**, 1157 (1985).

<sup>9</sup>R. Ludeke, T.-C. Chiang, and T. Miller, *J. Vac. Sci. Technol. B* **1**, 581 (1983).

<sup>10</sup>L. J. Brillson, *J. Vac. Sci. Technol.* **16**, 1137 (1979).

<sup>11</sup>J. L. Freeouf and J. M. Woodall, *Appl. Phys. Lett.* **39**, 727 (1981).

<sup>12</sup>J. M. Woodall and J. L. Freeouf, *J. Vac. Sci. Technol.* **19**, 794 (1981).

<sup>13</sup>R. H. Williams, V. Montgomery, and R. R. Varma, *J. Phys. Chem.* **11**, L735 (1978); V. Montgomery, R. H. Williams, and G. P. Srivastava, *ibid.* **14**, L191 (1981).

<sup>14</sup>L. J. Brillson, C. F. Brucker, A. D. Katnami, N. G. Stoffel, and G. Margaritondo, *Appl. Phys. Lett.* **38**, 784 (1981); C. F. Brucker and L. J. Brillson, *ibid.* **39**, 67 (1981).

<sup>15</sup>R. W. Grant, J. R. Waldrop, S. P. Kowalczyk, and E. A. Kraut, *J. Vac. Sci. Technol.* **19**, 477 (1981).

<sup>16</sup>W. E. Spicer and S. J. Eglash, in *VLSI Electronics: Microstructure Science* (Academic, New York, 1985), Vol. 10, p. 79.

<sup>17</sup>M. S. Daw and D. L. Smith, *Appl. Phys. Lett.* **8**, 690 (1980).

<sup>18</sup>R. E. Allen and J. D. Dow, *Phys. Rev. B* **25**, 1423 (1982).

<sup>19</sup>R. E. Allen, T. J. Humphreys, J. D. Dow, and O. F. Sankey, *J. Vac. Sci. Technol. B* **2**, 449 (1984).

<sup>20</sup>O. F. Sankey, R. E. Allen, S.-F. Ren, and J. D. Dow, *J. Vac. Sci. Technol. B* **3**, 1162 (1985).

<sup>21</sup>K. Kajiyama, Y. Mizushima, and S. Sakata, *Appl. Phys. Lett.* **23**, 458 (1973).

<sup>22</sup>H. H. Wieder, *Appl. Phys. Lett.* **38**, 170 (1981).

<sup>23</sup>L. J. Brillson, M. L. Slade, R. E. Viturro, M. Kelly, N. Tache, G. Margaritondo, J. M. Woodall, P. D. Kirchner, G. D. Pettit, and S. L. Wright (unpublished).

<sup>24</sup>R. Z. Bachrach, R. S. Bauer, P. Chiaradia, and G. V. Hansson, *J. Vac. Sci. Technol.* **18**, 797 (1981).

<sup>25</sup>M. P. Seah and W. A. Dench, *Surf. Interface Anal.* **1**, 2 (1979).

<sup>26</sup>E. W. Williams and V. Rehn, *Phys. Rev.* **172**, 798 (1969).

<sup>27</sup>H.-U. Baier, L. Koenders, and W. Mönch, *J. Vac. Sci. Technol. B* **4**, 1095 (1986).

<sup>28</sup>P. Chiaradia, A. D. Katnami, H. W. Sang, Jr., and R. S. Bauer, *Phys. Rev. Lett.* **52**, 1246 (1984).

<sup>29</sup>J. van Laar, A. Huijser, and T. L. van Rooy, *J. Vac. Sci. Technol.* **14**, 894 (1977).

<sup>30</sup>R. R. Daniels, T.-X. Zhao, and G. Margaritondo, *J. Vac. Sci. Technol. A* **2**, 831 (1984).

<sup>31</sup>K. H. Hsieh, M. Hollis, G. Wicks, C. E. Wood, and L. F. Eastman, *Inst. Phys. Conf. Ser.* **65**, 165 (1983).

<sup>32</sup>J. O. McCaldin, T. C. McGill, and C. A. Mead, *Phys. Rev. Lett.* **36**, 56 (1976).

<sup>33</sup>A. Nedoluha, *J. Vac. Sci. Technol.* **21**, 429 (1982).

<sup>34</sup>H. H. Weider, A. R. Clawson, D. I. Elder, and D. A. Collins, *IEEE Electron Device Lett.* **EDL-2**, 73 (1981).

<sup>35</sup>H. H. Weider, *Surf. Sci.* **132**, 390 (1983).

<sup>36</sup>H. B. Michaelson, *J. Appl. Phys.* **48**, 4729 (1977), and references therein.